Journal of Industrial and Engineering Chemistry 138 (2024) 332–337

Contents lists available at ScienceDirect

Journal of Industrial and Engineering Chemistry

journal homepage: www.elsevier.com/locate/jiec

Full Length Article

Development of biodegradable bag materials as a sustainable alternative to conventional plastic bags

WooSeok Lee [a,b], Tai Gyu Lee [a,b,*]

[a] Department of Chemical and Biomolecular Engineering, Yonsei University, 50 Yonsei-ro, Seodaemun-gu, Seoul 03722, Republic of Korea
[b] Korean Association of Biodegradable Plastic Ecosystem, 42 Insa-dong 5-gil, Jongno-gu, Seoul 03149, Republic of Korea

ARTICLE INFO

Keywords:
Biodegradable
Plastic bag
Natural polymer
Sodium alginate
Stearic acid

ABSTRACT

Biodegradable plastics are actively studied to address the environmental issues caused by petroleum-based plastics. Sodium-alginate-based biodegradable materials containing crosslinking agents and stearic acid have been developed. A sodium alginate-based bag was fabricated by immersing a film composed of sodium alginate and stearic acid into a calcium lactic acid solution, to induce transformation through calcium bonding. These bags exhibited variations in tensile strength (TS), breaking height (E), moisture absorption, swelling, and contact angle depending on the percentage of stearic acid (1, 3, 5, 8, and 10 %); additionally, stearic acid showed a rough surface in morphological measurements. The rough surface facilitated effective integration with stearic acid, ultimately improving hydrophobicity. This was confirmed by a water absorption experiment. In addition, the combination of stearic acid and sodium alginate resulted in an increased breaking height, demonstrating comparable performance to conventional plastic bag. The interaction between sodium alginate and stearic acid shows that the generated biodegradable bags exhibit physical properties similar to those of the conventional plastic bags.

Introduction

Plastic products, such as disposable items, packaging materials, and toys, are encountered almost on a daily basis across a multitude of industries, ranging from construction to automotive sectors [1–3]. The rapid increase in the production and consumption of plastics has raised global concerns regarding plastic waste management. Current plastic waste disposal methods such as incineration and landfilling have adverse environmental impacts [4]. Among disposable plastics, garbage bags are typically processed in treatment facilities, where they are removed via a process that may not always ensure complete removal, potentially resulting in fine plastic residues [5]. Consequently, biodegradable polymers with properties similar to those of conventional plastics have been proposed as alternatives. Anaerobic digestion (AD) of bags and bioplastics has garnered significant interest because AD can potentially generate methane (CH_4), a source of renewable energy [6].

Biodegradable bags, which exhibit properties similar to those of conventional plastics, are used for garbage management. These bags can be used to transport organic garbage and can be left in soil or composting pits with adequate aeration. Such bags do not leave harmful toxic residues in the environment and can biodegrade within several months [7–9]. Natural polymers are naturally extracted, biodegradable, and are in the spotlight as fossil fuel-based plastic alternatives [9]. Sodium alginate, which is a natural polymer, is extracted from brown algae and consists of a chain of β-D-mannuronic acid (M) and α-L-guluronic acid (G) units linked by glycosidic (1–4) bonds. Sodium alginate is used in various industries because of its biodegradability and renewability [10]. Given the inherent characteristics of natural polymers, improving their mechanical properties and tensile strength is essential, often necessitating the use of plasticizers or cross-linkers [11,12].

Cross-linkers such as acids, amines, epoxy resins, and metal salts are used to enhance the mechanical properties of polymers [13]. Sodium alginate can react with divalent and trivalent cations, especially calcium ions. Gelling by Ca^{2+} occurs due to the specific and powerful interaction between the G block of sodium alginate and Ca^{2+}, resulting in the formation of an egg box structure [14–16]. The crosslinking of sodium alginate and Ca^{2+} could improve the mechanical properties of sodium alginate[17]. Volatile fatty acids can be used as crosslinking agents and can be used to generate biopolymers with mechanical and thermal properties comparable to fossil fuel-based plastics [18].

* Corresponding author at: Department of Chemical and Biomolecular Engineering, Yonsei University, 50 Yonsei-ro, Seodaemun-gu, Seoul 03722, Republic of Korea.
E-mail address: teddy.lee@yonsei.ac.kr (T.G. Lee).

https://doi.org/10.1016/j.jiec.2024.04.009
Received 15 February 2024; Received in revised form 2 April 2024; Accepted 6 April 2024
Available online 7 April 2024

In this study, stearic acid was used to improve the mechanical strength because of its biodegradability and its capability to enhance the moisture barrier properties of starch films [19]. Moreover, many composite films fabricated by combining hydrophobic lipid compounds with hydrophilic structural matrices have exhibited improved moisture resistance [14]. Plasticizers, which are low-molecular-weight substances used to fill the gaps between polymer chains, enhance flexibility, tensile strength, and ductility. Glycerol, xylitol, and sugars are commonly used as plasticizers owing to their compatibility with polymers. Among these, glycerol has been reported as the most effective plasticizer for improving the moisture content and mechanical properties in numerous studies [20,21].

In previous studies, many studies have been conducted to replace fossil fuel-based plastics using sodium alginate. However, due to the limitations of mechanical and chemical properties of sodium alginate, it was not suitable for practical application. In this experiment, an improved bags material was produced by crosslinking sodium alginate and stearic acid in a simple way, and the experiment was conducted by measuring the physical properties and compared with commercially used bags. An aqueous solution of sodium alginate with an appropriate solid content was crosslinked with stearic acid and plasticized with glycerol to effectively enhance its properties. Furthermore, calcium ions were introduced through immersion in a calcium lactate solution to improve the weak properties of sodium alginate and render it suitable for use as a bag material.

The effects of these components were confirmed through FT-IR (Fourier transform infrared) spectroscopy, morphology, mechanical properties, water properties including moisture content and contact angle measurement, thermal properties, and BOD (Biological Oxygen Demand) measurement.

Materials and methods

Chemicals and reagents

The reagents and chemicals used in this study are as follows. Sodium alginate, the primary precursor used in the bags, was purchased from Junsei (Tokyo, Japan). Stearic acid was obtained from Samchun (Gangnam-gu, Seoul, South Korea). Ethanol was purchased from Dajung Chemical Co., Ltd. Distilled water was used as received, without further purification.

Preparation of sodium alginate bag samples

In this chapter, the proper crosslinking of stearic acid with sodium alginate has been to investigated to improve the film formed by the ionic bonding of sodium alginate and calcium via the previous experiment, which was characterized as too weak to be used as SAB. Stearic acid, being a fatty acid, has a limited ability to interact with water and exhibits limited solubility in water because of its low water solubility [22,23]. Therefore, crosslinking stearic acid with sodium alginate can protect other materials from moisture.

A sodium alginate bag (SAB) was prepared using the solution-casting method. First, the crosslinking agent, stearic acid, was introduced into ethanol, and the concentration of stearic acid was adjusted to 0, 1, 3, 5, 8, and 10 %. After complete dissolution, the solution was mixed with distilled water to obtain the solvent. It was then heated to 60 °C using an SMHS-3 hotplate stirrer (DAIHAN Scientific Co., Ltd., South Korea). Subsequently, 3 % (w/v) of sodium alginate was added, and the mixture was stirred for 3 h at a constant temperature. The solution was cast into a plastic tray (300 × 225 × h 42 mm) at a thickness of 30 mm and dried for 8 h in a convection oven, at 50 °C. Subsequently, the dried sodium alginate film was immersed in a 5 % (w/v) calcium lactate solution, prepared by dissolving calcium lactate in distilled water, for 2 min. The film was removed and air-dried at room temperature for 8 h. The dried SAB was cut into appropriate sizes and sealed in bags for storage. Formulations used in this study are listed in Table 1.

Fourier transform infrared (FT-IR) spectroscopy

A Fourier transform infrared (FT-IR) spectrometer (Vertex70 spectrometer; Bruker, Germany) was used to confirm the variations in the physical and chemical properties and interactions of SAS according to the components. Each SAS spectrum was analyzed within the range of 3500 to 800 cm^{-1} at a resolution of 4 cm^{-1}, with each scan comprising 32 scans.

Morphology

The microstructure of SAS was observed using a field-emission scanning electron microscope (JEOL-7800F) (JEOL Ltd., USA). The surface and cross-section of each sample were affixed to a support, coated with platinum 60 s prior to image observation, and measured at an acceleration voltage of 2.00–10.00 kV. The surface was measured at 10,000× magnification, and the cross-section was measured at 5,000× magnification.

Mechanical property

The elongation and tensile strength were measured using a universal testing machine (UTM, LR10K, Lloyd Instruments, Ltd., UK). The SAS thickness was measured using a Mitutoyo absolute digital caliper (Mitutoyo Corp, Kanogawa, Japan), and the thickness of the prepared SAS at five points was averaged. The test was based on the American Society of Testing Materials (ASTM) D882, and the test was repeated more than five times for each sample, at a rate of 50 mm/min at room temperature.

Moisture properties

Moisture absorption and swelling are important indicators for the use of plastic Bags. Each SAS was randomly selected, and the weight (W_d) of the initial dry state was measured.

The samples were then immersed in distilled water at room temperature for 10 min. Subsequently, excess water was wiped off the surface using Kimtech to prevent it from flowing, and the weight (W_s) was measured. The degree of absorption and swelling were calculated according to formulas 1 and 2. For each sample, we used the average value of at least three iterations.

$$Waterabsorption = \frac{W_s - W_d}{W_s} \times 100 \quad (1)$$

$$Waterswellingratio = \frac{W_s - W_d}{W_d} \times 100 \quad (2)$$

The contact angle was measured using the session drop mode of a contact angle analyzer (Attension-Biolin Scientific AB, Sweden). A 2*2 cm SAS was placed on a horizontal Teflon plate, and 10 uL of distilled water was dropped onto the surface using a micro cylinder. Each sample was evaluated more than three times, and the average value was calculated using a contact angle analyzer.

Thermal property

Thermal property was measured using a TA instrument Q50 (TA

Table 1
Codes used in the formulations of SA and stearic acid.

SA content (% w/w)	Stearic acid (%)					
	0	1	3	5	8	10
3	0 SAS	1 SAS	3 SAS	5 SAS	8 SAS	10 SAS

Instruments, New Castle, DE, USA). 10 mg of each sample was charged and heated to 40–600 °C, at a rate of 10 °C/min under an oxygen flow.

Biodegradability

BOD measurements were conducted to confirm biodegradability. The prepared sample was stirred in a phosphate-buffered saline (PBS) solution for 7 days in an incubator at a temperature of 50 °C and humidity of 55 %. The degree of biodegradation was identified by analyzing the amount of carbon dioxide generated. BOD was measured with reference to ISO 14851. A sample was cultured in a sealed bottle after preparing a solution by collecting the soil under the Yonsei University tree. The amount of carbon dioxide generated over time between cellulose and SAS, which are representative biodegradable materials, was measured.

Results and discussion

Fourier transform infrared (FT-IR) spectroscopy

The FT-IR spectra for each SA additive ratio are shown in Fig. 1. The FT-IR spectra as a function of stearic acid content in SA are shown in the regions of 3500–2400 cm^{-1} (Fig. 1 a) and 2400–800 cm^{-1} (Fig. 1 b). The changes were mainly due to stearic acid addition; a broad band around 3000 bands was attributed to hydroxyl groups (–OH) and free water content [12,24,25]. This peak was attributed to the interaction between hydroxide groups and sodium alginate [26]. From previous results, the O–H stretching vibration of sodium alginate, aliphatic C–H stretching vibration, and aliphatic C–H stretching vibration were observed at ~ 3200, 2900, and 2925 cm^{-1}, respectively, and COO stretching was observed at 1600 and 1400 cm^{-1}. The sharp peak at 1100 cm^{-1} is associated with C–O, C–C, and CO–C stretching vibrations.

Sodium alginate ionized by calcium lactate showed peaks similar to that in the FT-IR spectrum of sodium alginate, where the stretching vibration absorption region of the hydroxyl bond was broader than that of calcium alginate because of the formation of a chelate structure on the calcium ion by the carboxyl group. This confirmed that the calcium in calcium lactate was properly ionized with sodium alginate. When comparing 0 SAO with 1, 3, 5, 8, and 10 SAO, a new peak was observed at 1740 cm^{-1}, which confirmed that the stearate group of stearic acid was bound to the sodium alginate polymer. In addition, the band of the hydroxyl group (OH) at 3200 cm^{-1} weakened with an increase in the amount of stearic acid, indicating the enhancement in moisture sensitivity.

Morphology

The SAS surface shown in Fig. 2 exhibits a uniform, continuous, and dense structure, formed by the interfacial adhesion between the components. 0 SAS exhibited a smooth and dense structure, confirming the irrelevancy of the surface modification of the SA films due to ionic bonding. In addition, the surface roughness of 1, 3, 5, 8, and 10 SAS increased with increasing stearic acid content. This is because the film morphology changed significantly upon the addition of fatty acids, resulting in a rough, uneven, and spotty white surface [27]. A rough surface can reduce the interaction with polar substances, such as water, and the change in surface energy can also increase hydrophobicity.

In conclusion, an increase in stearic acid content led to an increase in surface roughness owing to the fatty acids on the surface, which in turn reduced the interaction with water, resulting in an increase in hydrophobicity.

Mechanical property

Table 2 lists the tensile strengths, elongations, and thicknesses of the SAS samples. Fig. 3 shows that the strength increased depending on whether stearic acid was added; however, elongation tended to decrease as the stearic acid content increased, owing to the interaction between stearic acid and sodium alginate caused by a decrease in the hydrogen bonds present in sodium alginate; similar results have been reported.

The increase in the tensile strength of stearic acid can be confirmed by the effective uniform integration of stearic acid into the polymer matrix of sodium alginate. In addition, when comparing the tensile strength and elongation of the SA sample in which only sodium alginate

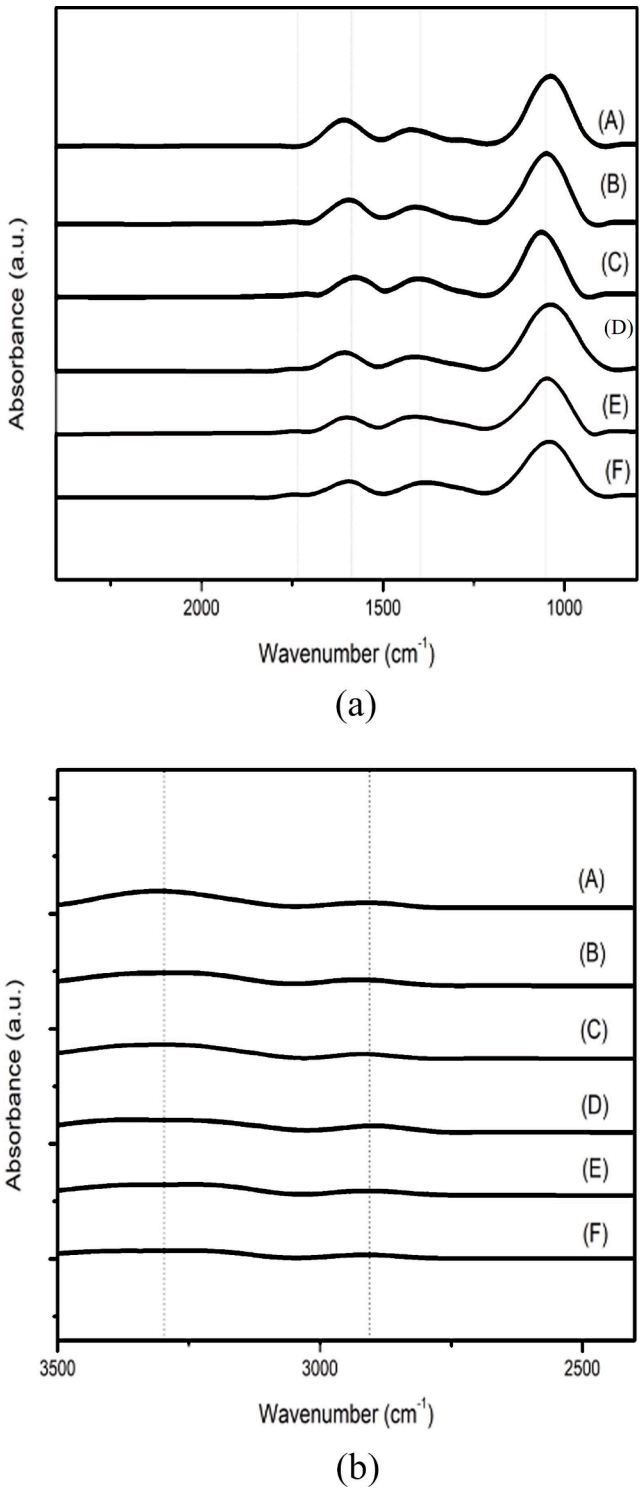

Fig. 1. FT-IR spectra of SAS (a) from 2400 to 800 cm^{-1} and (b) from 3500 to 2400 cm^{-1} ((A) 0 SAS, (B) 1 SAS, (C) 3 SAS, (D) 5 SAS, (E) 8 SAS, and (F) 10 SAS).

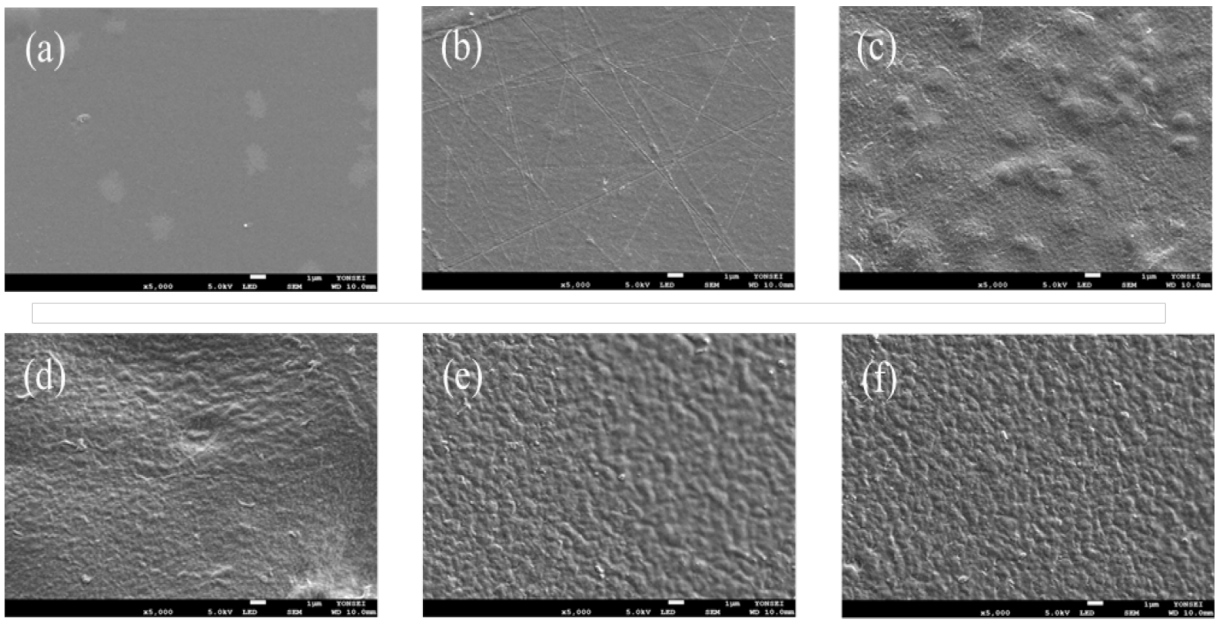

Fig. 2. Microstructure and surface morphology of the formulated SAS by SEM: (a) 0 SAS, (b) 1 SAS, (c) 3 SAS, (d) 5 SAS, (e) 8 SAS, and (f) 10 SAS.

Table 2
Thickness, strength, and elongation of SAS.

Formulation	Thickness(mm)	Strength (Mpa)	Elongation (%)
0 SAS	0.041 ± 0.003	20.01 ± 5.00	16.08 ± 3.02
1 SAS	0.045 ± 0.004	21.77 ± 8.06	15.04 ± 2.48
3 SAS	0.067 ± 0.006	25.84 ± 4.26	13.19 ± 3.47
5 SAS	0.096 ± 0.004	26.06 ± 1.64	13.56 ± 5.13
8 SAS	1.04 ± 0.002	30.95 ± 7.19	12.67 ± 3.76
10 SAS	1.16 ± 0.003	38.18 ± 4.59	12.38 ± 0.86

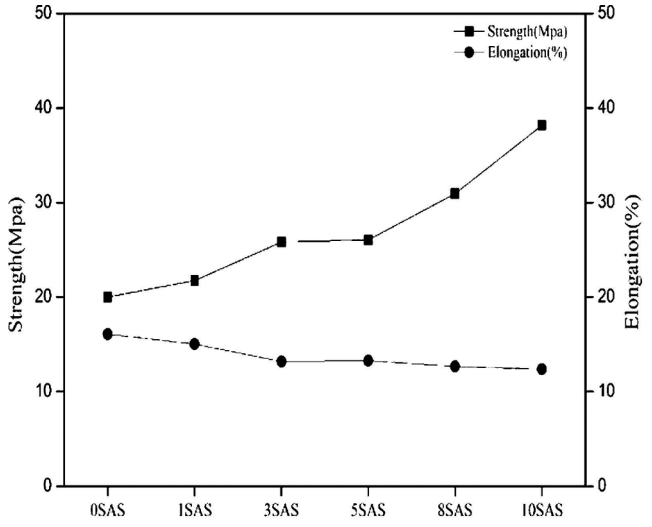

Fig. 3. Tensile strength (Mpa) and elongation (%) of SAS.

and calcium are combined, the tensile strength and elongation of the SAS sample are higher. It was confirmed that the physical properties were improved due to the crosslinking of stearic acid [17]. This resulted in an increased network resistance, as confirmed by the decrease in flexibility owing to the formation of a strong matrix on the matrix of stearic acid and sodium alginate. This confirms the increase in tensile strength due to the uniform binding of sodium alginate and stearic acid [27].

In comparative analysis of the mechanical properties between the SA sample, consisting solely of sodium alginate and calcium, and the SAS sample, which incorporates sodium alginate, calcium, and stearic acid, we observed a marked enhancement in both tensile strength and elongation for the SAS sample. This improvement can be attributed to the crosslinking effects introduced by the incorporation of stearic acid, which significantly bolster the sample's mechanical properties.

The tensile strength of the 10SAS bags, reaching a maximum of 38.18 MPa, aligns with or surpasses that of commercial fossil fuel-based polyethylene bags, where high-density polyethylene (HDPE) generally exhibits tensile strengths ranging from 20 to 40 MPa, and low-density polyethylene (LDPE) shows values between 10 and 30 MPa. Nevertheless, the elongation at break for the 10SAS bags, recorded at 12.38 %, falls significantly short of the typical ranges of 100 % to 700 % for LDPE and 100 % to 300 % for HDPE bags, underscoring a notable deficit in flexibility.

This comparison demonstrates that while the 10SAS bags can match or exceed the mechanical strength of conventional plastic bags, their lower elongation rate confirms a reduced capacity for deformation, highlighting a diminished adaptability for certain applications due to their lower elongation.

Moisture properties

Table 3 shows the contact angles of SAS according to the stearic acid ratio. The contact angle is a basic wetting property that indicates the degree of hydrophilicity and hydrophobicity. When the contact angle of a surface is 65° or less, it is generally considered hydrophilic. The interactions between the substances after blending were analyzed based on the contact angles. The contact angle was lowest for 0 SAS (25.44°)

Table 3
Moisture properties of SAS.

Film	Water absorption (%)	Water swelling (%)	Water contact angle (°)
0 SAS	68.61 ± 8.48	218.53 ± 14.82	25.44 ± 5.53
1 SAS	65.89 ± 9.06	193.18 ± 12.17	28.87 ± 3.61
3 SAS	63.74 ± 6.53	175.75 ± 14.64	40.55 ± 6.11
5 SAS	59.63 ± 6.59	147.67 ± 10.87	65.41 ± 5.34
8 SAS	55.56 ± 3.62	125.22 ± 11.25	72.19 ± 1.26
10 SAS	50.86 ± 6.68	103.50 ± 10.28	87.73 ± 7.88

and highest for 10 SAS (87.73°). Table 3 shows that the SAB films of 0, 1, and 3 SAS had contact angles of less than 65°, and the SAB films of 5, 8, and 10 SAS had contact angles greater than 65°, indicating the increase in hydrophobicity owing to the addition of stearic acid.

The results of previous experiments confirmed that the surface of SAB became uneven and rough with increasing stearic acid content. This occurrence can be attributed to the formation of a cohesive network between the sodium alginate polymer and stearic acid. This phenomenon is closely associated with the observed increase in contact angle (which changes with roughness), owing to the changes in the wetness model governing the interaction between the water droplets and surface [26–30]. The rough surface resulting from the increase in the stearic acid content reduces the contact area between solids and liquids, ultimately resulting in an increase in the water contact angle.

Thermal property

Fig. 4 shows the decomposition behavior and thermal stability of the SAB film using a thermogravimetric (TG) curve. The reduction in the sample mass was related to the thermal decomposition of the components. This caused the SAS graphs to differ from each other. All raw materials and complexes exhibited varying stages of reduction and thermally decomposed in the presence or absence of stearic acid, with decomposition occurring within a range of temperatures rather than at a specific temperature. The first degradation was due to the dehydration of water and low molecular weight materials that were loosely bound at 30–180 °C. The second decomposition occurred at 200–230 °C and contributed to a weight reduction of 36 % for 0 SAS, with approximately 20 % due to the addition of stearic acid formed by the decomposition of sodium alginate [22].

Decomposition temperatures varied in the range of 211–235 °C, based on the stearic acid content. Furthermore, a gentle reduction curve, due to the stearic acid content, was observed at 240–510 °C. The gentle curve confirmed that the thermal stability increased because of the binding with stearic acid [31–35].

Finally, complete combustion by oxygen occurred around 580 °C [27]. The analysis showed that the decomposition temperature of SAS increased as the stearic acid content increased. Furthermore, weight loss exhibited a gradual reduction curve after the first reduction, compared with the 0 SAS sample. This suggests that stearic acid mixed well with sodium alginate and slowed oxidation.

Biodegradability

The amount of carbon dioxide generated over time between cellulose and SAS, which are representative biodegradable materials, was measured. Fig. 5 shows the amount of carbon dioxide generated over time between cellulose and 10 SAS. The cultured SAS sample was not visible because of decomposition, which was later confirmed to be hydrolysis.

Cellulose exhibited a constant increase in the carbon dioxide content over time, and 10 SAS produced more carbon dioxide than cellulose after 24 h. Thus, 10 SAS, which was produced by cross-linking with stearic acid, was confirmed to biodegrade faster than cellulose, with 100 % biodegradability.

Conclusions

A SAB was successfully fabricated by forming a film via solution casting and calcium ion bonding with calcium lactate. To compensate for its weak mechanical properties, the chemical structure, mechanical properties, shape, thermal properties, and water resistance of films, manufactured by crosslinking with stearic acid, were evaluated.

Tensile strength increased proportional to the amount of stearic acid added, and the formation of a cohesive network of sodium alginate and stearic acid was confirmed by a decrease in elongation. FT-IR spectroscopy confirmed the effect of the presence or absence of binding with stearic acid and reduction of carbonyl groups on the improvement of the moisture-weak properties. The surface change and contact angle confirmed the improvement in hydrophobicity owing to the increase in the contact angle as the surface became rough. Furthermore, the manufactured SAB material completely burned under oxygen conditions, resulting in different results depending on the components. Moreover, the material exhibited 100 % natural decomposition potential owing to its thermal properties.

As the concentration of stearic acid combined with sodium alginate increased, the weight loss due to free moisture decreased. Additionally, an increase in the stearic acid concentration prevented oxidation. In conclusion, a bag that can be placed in an envelope and discarded without any separate removal process was developed.

Furthermore, the properties of stearic acid dissolved in organic solvents presents a promising avenue for addressing the issue of biodegradation time control, often encountered with existing biodegradable plastics. This study suggests that this 100 % naturally decomposable material hold significant potential for use in various applications, beyond bags.

Funding

This research did not receive any specific grant from funding agencies in the public, commercial, or not-for-profit sectors.

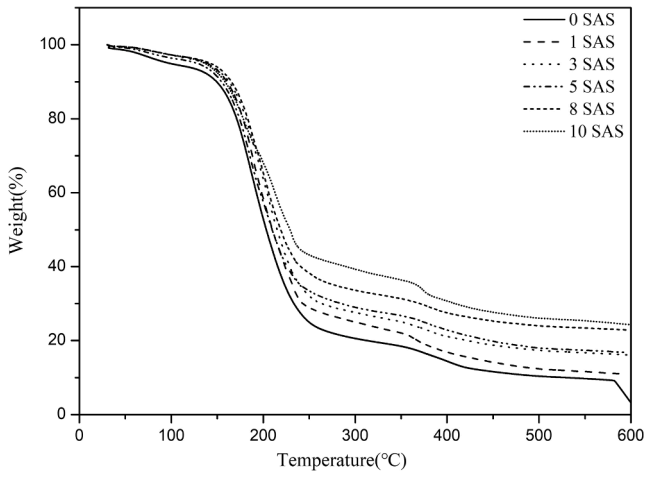

Fig. 4. TGA curves of the SAB formulated with different stearic acid contents.

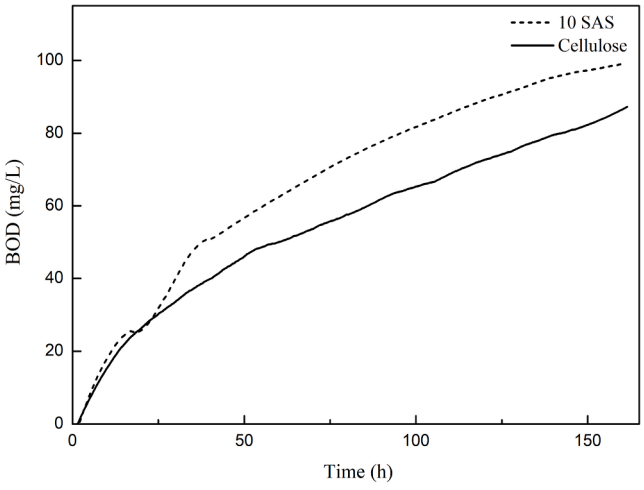

Fig. 5. Measurement of the BOD of cellulose and 10 SAS film.

CRediT authorship contribution statement

WooSeok Lee: Writing – original draft, Writing – review & editing. **Tai Gyu Lee:** Writing – original draft, Writing – review & editing.

Declaration of competing interest

The authors declare that they have no known competing financial interests or personal relationship that could appeared to influence the work reported in this paper.

Acknowledgements

This work is financially supported by Korea Ministry of Environment (MOE) Graduate School specialized in Integrated Pollution Prevention and Control Project.

References

[1] J.P. Reddy, J.W. Rhim, Carbohydr. Polym. 110 (2014) 480–488, https://doi.org/10.1016/j.carbpol.2014.04.056.
[2] S. Mohajer, M. Rezaei, S.F. Hosseini, 157 (2017) 784-793. Doi: 10.1016/j.carbpol.2016.10.061.
[3] T.J. Madera-Santana, Y.F. Pelegrín, J.A. Azamar-Barrios, Int. J. Biol. Macromol. 69 (2014) 176–184, https://doi.org/10.1016/j.ijbiomac.2014.05.044.
[4] R. Jumaidin, S.M. Sapuan, M. Jawaid, M.R. Ishak, J. Sahari, Int. J. Biol. Macromol. 97 (2017) 606–615, https://doi.org/10.1016/j.ijbiomac.2017.01.079.
[5] J.S. Park, H.S. Joo, J.Y. Ryu, C.G. Phae, Y.S. Jeon, J. Korea Org. Resources Recycling Assoc. 10 (1) (2002) 109–119.
[6] J.H. Kang, S.W. Kang, W.J. Kim, D.H. Kim, S.W. Im, Fermentation 8 (11) (2022) 638, https://doi.org/10.3390/fermentation8110638.
[7] M. Brodhagen, J.R. Goldberger, D.G. Hayes, D.A. Inglis, T.L. Marsh, C. Miles, Environ Sci Policy 69 (2017) 81–84, https://doi.org/10.1016/j.envsci.2016.12.014.
[8] M. Narodoslawsky, K. Shazad, R. Kollmann, H. Schnitzer, Chem. Biochem. Eng. Q. 29 (2015) 299–305, https://doi.org/10.15255/CABEQ.2014.2262.
[9] A. Dirpan, A.F. Ainani, M. Djalal, Polymers 15 (13) (2023) 2781, https://doi.org/10.3390/polym15132781.
[10] H. Yagi, F. Ninomiya, M. Funabashi, M. Kunioka, Polym. Degrad. Stab. 110 (2014) 278–283, https://doi.org/10.1016/j.polymdegradstab.2014.08.031.
[11] R.A. Khajouei, L. Tounsi, N. Shahabi, A.K. Patel, S. Abdelkafi, P. Michaud, Mar. Drugs 20 (6) (2022) 364, https://doi.org/10.3390/md20060364.
[12] S. Shankar, J.P. Reddy, J.W. Rhim, Int. J. Biol. Macromol. 81 (2015) 267–273, https://doi.org/10.1016/j.ijbiomac.2015.08.015.
[13] Y. Wu, F. Geng, P.R. Chang, J. Yu, X. Ma, Carbohydr. Polym. 76 (2) (2009) 299–304, https://doi.org/10.1016/j.carbpol.2008.10.031.
[14] M.B. Nieto, Edible Food Packaging Materials and Processing Technologies, CRC Press, Boca Raton, 2016, pp. 9–79.
[15] J.W. Rhim, LWT-Food Sci. Technol. 37 (3) (2004) 323–330, https://doi.org/10.1016/j.lwt.2003.09.008.
[16] J. Yoon, D.X. Oh, C. Jo, J. Lee, D.S. Hwang, PCCP 16 (46) (2014) 25628–25635, https://doi.org/10.1039/C4CP03499F.
[17] S.F. Bt Ibrahim, N.A.N. Mohd Azam, K.A. Mat Amin, Mater. Sci. Eng. 509 (2019) 012063. 10.1088/1757-899X/509/1/012063.
[18] C. Amabile, T. Abate, C. De Crescenzo, R. Muñoz, S. Chianese, D. Musmarra, Chem. Eng. J. 473 (2023) 145193, https://doi.org/10.1016/j.cej.2023.145193.
[19] C. Araki, S. Hirase, Bull. Chem. Soc. Jpn. 26 (1953) 463–467.
[20] K.C. Labropoulos, D.E. Niesz, S.C. Danforth, P.G. Kevrekidis, Carbohydr. Polym. 50 (4) (2002) 393–406, https://doi.org/10.1016/S0144-8617(02)00084-X.
[21] L. Cabedo, J.L. Feijoo, V.M. Pilar, J.M. Lagarón, E. Giménez, Macromol. Symp. 233 (1) (2006) 191–197, https://doi.org/10.1002/masy.200690017.
[22] A. Sorrentino, G. Gorrasi, V. Vittoria, Trends Food Sci. Technol. 18 (2) (2007) 84–95, https://doi.org/10.1016/j.tifs.2006.09.004.
[23] M.A. García, M.N. Martino, N.E. Zaritzky, Starch - Stärke 52 (4) (2000) 118–124, https://doi.org/10.1002/1521-379X(200006)52:4<118::AID-STAR118>3.0.CO;2-0.
[24] R.A. Talja, H. Helén, Y.H. Roos, K. Jouppila, Carbohydr. Polym. 67 (3) (2007) 288–295, https://doi.org/10.1016/j.carbpol.2006.05.019.
[25] K. Ciardullo, E. Donner, M.R. Thompson, Q. Liu, Starch-Stärke 71 (7–8) (2019) 1800196, https://doi.org/10.1002/star.201800196.
[26] P.C. Srinivasa, M.N. Ramesh, R.N. Tharanathan, Food Hydrocoll. 21 (7) (2007) 1113–1122, https://doi.org/10.1016/j.foodhyd.2006.08.005.
[27] P.I. Campa-Siqueiros, I. Vargas-Arispuro, P. Quintana-Owen, Y. Freile-Pelegrín, J. A. Azamar-Barrios, T.J. Madera-Santana, Int. J. Biol. Macromol. 151 (2020) 27–35, https://doi.org/10.1016/j.ijbiomac.2020.02.158.
[28] R. Jumaidin, S.M. Sapuan, M. Jawaid, M.R. Ishak, Int. J. Biol. Macromol. 97 (2017), https://doi.org/10.1016/j.ijbiomac.2017.01.079.
[29] L.C. Bertan, F.M. Fakhouri, A.C. Siani, C.R. Ferreira Rosso, Macromolecular Symposia 229 (1) (2005) 143–149, https://doi.org/10.1002/masy.200551117.
[30] M. He, M. Xu, L. Zhang, ACS Appl. Mater. Interfaces 5 (2013) 585–591, https://doi.org/10.1021/am3026536.
[31] N. Garoff, S. Zauscher, Langmuir 18 (18) (2002) 6921–6927, https://doi.org/10.1021/la025787g.
[32] K.J. Kubiak, M.C. Wilson, T.G. Mathia, P. Carval, Wear 271 (2011) 523–528, https://doi.org/10.1016/j.wear.2010.03.029.
[33] P. Cerruti, G. Santagata, G.G. d'Ayala, V. Ambrogi, C. Carfagna, M. Malinconico, P. Persico, Degradation and Stability 96(5) (2011) 839-846. Doi: 10.1016/j.polymdegradstab.2011.02.003.
[34] S.W. Hwang, J.K. Shim, S. Selke, H. Soto-Valdez, L. Matuana, M. Rubino, R. Auras, J. Food Eng. 116 (4) (2013) 814–828, https://doi.org/10.1016/j.jfoodeng.2013.01.032.
[35] S. Mathew, T.E. Abraham, Food Hydrocoll. 22 (5) (2008) 826–835, https://doi.org/10.1016/j.foodhyd.2007.03.012.